

Supporting Information

Dehydrogenase *versus* oxidase function: the interplay between substrate binding and flavin microenvironment

Teresa Benedetta Guerriere¹, Alessandro Vancheri², Ilaria Ricotti², Stefano A Serapian², Daniel Eggerichs³, Dirk Tischler³, Giorgio Colombo², Maria L. Mascotti⁴, Marco W. Fraaije^{5*}, Andrea Mattevi^{1*}

¹Department of Biology and Biotechnology “Lazzaro Spallanzani”, University of Pavia, Pavia, Italy 27100.

² Department of Chemistry, University of Pavia, 27100 Pavia, Italy

³ Microbial Biotechnology, Ruhr University Bochum, 44780, Bochum, Germany.

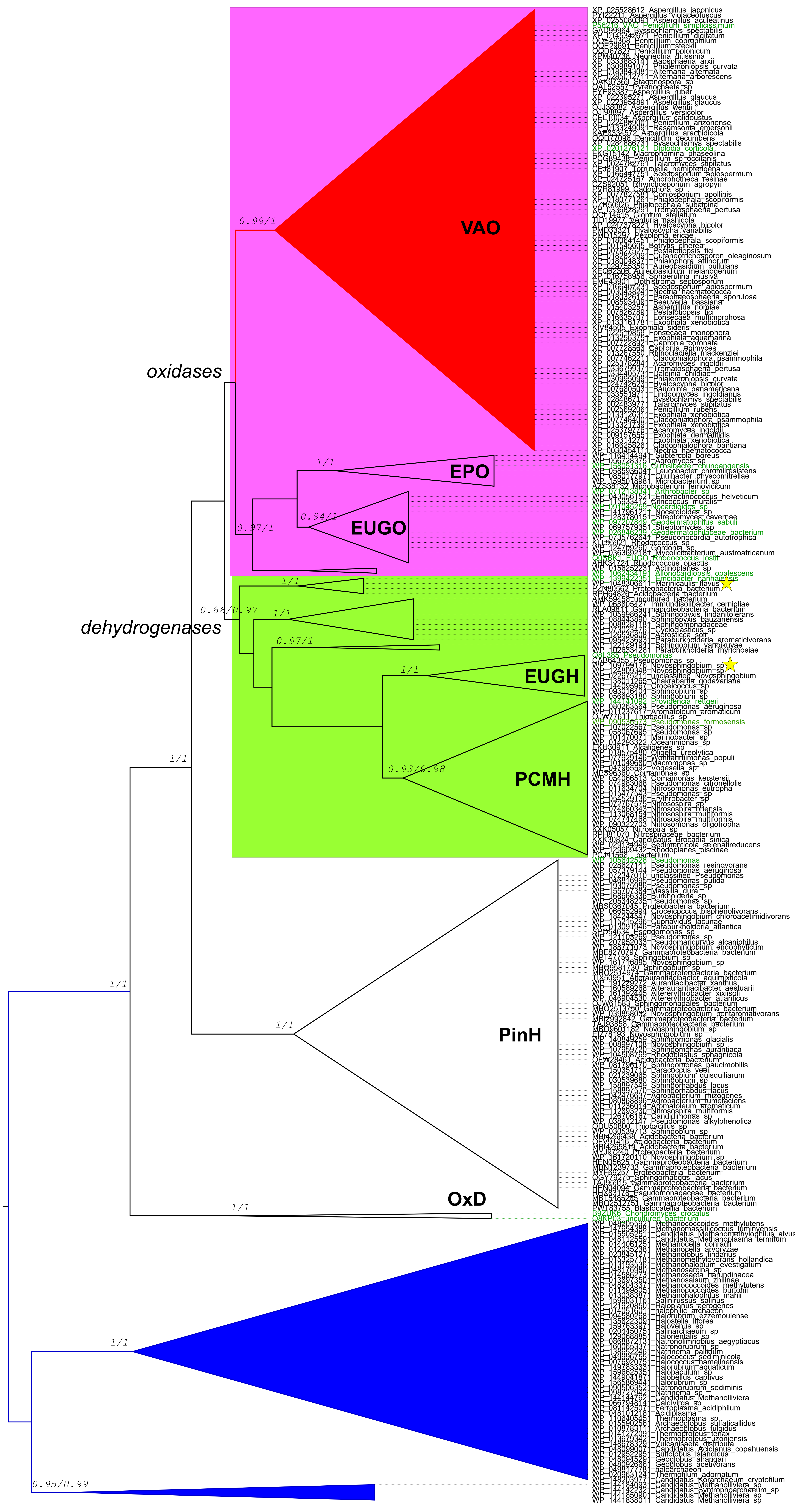
⁴ IHEM CONICET, Universidad Nacional de Cuyo, Mendoza, Argentina, M5502JMA.

⁵ Molecular Enzymology Group, University of Groningen, Groningen, The Netherlands, 9747AG.

***Correspondence:** M.W.Fraaije@rug.nl; andrea.mattevi@unipv.it

Table of Contents

Annotated phylogeny of the VAO/PCMH flavoprotein family (Figure S1)	S2
Sequence alignment and identities (Figure S2)	S4
Determination of the midpoint redox potential (Em) of VAD (Figure S3)	S6
Steady-state kinetics experiments on VAD (Figure S4)	S7
Steady-state kinetics experiments on nsVAO (Figure S5)	S9
Steady-state kinetics experiments on EUGO (Figure S6)	S9
Stopped-flow kinetics (Figure S7)	S10
Enzyme-monitored turnover experiment (Figure S8)	S11
The electron density of the flavin and surrounding residues in nsVAO (Figure S9)	S12
Properties of nsVAO T181D mutant (Figure S10)	S12
Data collection and refinement statistics (Table S1)	S13
Genetic context (Table S2)	S16
Steady state kinetic parameters of P151L VAD (Table S3)	S18
Primers used for quick change mutagenesis (Table S4)	S18



Supplementary Figure 1. Annotated phylogeny of the VAO/PCMH flavoprotein family. The tree was constructed in RAxML v8.2.10 using 500 rapid bootstraps and automated model selection. The Transfer Bootstrap Expectation/Poster Probability support values are shown at the nodes. Taxonomic groups are colored as follows: Fungi (red), Bacteria (white) and Archaea (blue). The accession codes and species name are given for each sequence included in the dataset. Experimentally characterized enzymes are shown in green. Clades are named as in the main text. The two sequences characterized in this work are marked with yellow stars. The scale bar indicates substitutions per site.

PinH	HGPKEQDPEFMALLGRGAKPEEYEAYAKKKGIPFWTCALTFYGPKEVKIRAQWEYAAQERFK	354
PCMH	-E-----PGHTPDSVIKQMOKDTGMGAWLTYAALYGTQEVDVNWKIVTDVFK	346
EUGH	-D-----PGPISEPDKAVFKELGIGYWNVYFALYGTAEQIAVNEKIVRSIIIE	344
nsVAO	-D-----GAPLDEASLKKAAASANGLGMWNTYFALYGTTEQTAVGVEPIIRATLT	372
VAO	-R-----TEPLSDEELDKIAKQLNLGRWNFYGALYGPPIRRLWETIKDAFS	376
VAD	-G-----DGPIPPSVAKTMMADLDLGWMNFCGALYGPPPVMDTLWTAIRDFA	340
EPO	-E-----PGPLTDEAKQRMVDELGIIGHIVYGTCTYGPWRQIDKYIEMIRDAYL	343
EUGO	-G-----DGPMMPAAIERMKKDLDLGFWNFYGTLGYGPPPLIEMYYGMIKEAFG	342
	. : * : **	
PinH	KAFPAKFAEHIFYKLPLTPEQA--EKVEYPAQFGIPNLRFTAIGARSNWNPAPPNGHA	412
PCMH	KL-GKGRIVTQEEAG----DTQPFKYRAQLMSGVPNLQEFGL--YNWRG--G-GGSM	393
EUGH	PS--GGEIVTEAEAG----DNILFLHHHKQLMCGETMMEEMNI--YRWRG--AGGGAC	391
nsVAO	AS--GGEVLTAAEEME----GNPWFHHHQTLMQGGLNLDEVGL--LRWRG--AGGLA	419
VAO	AI--PGVKFYFPEDTP----ENSVLVRDRKTMQGIPTYDELKW--IDWLP--N-GAHL	423
VAD	DI--PGVKFYFPEDRR----HKVDLLLHRAETMKGVPKLTFNF---LNWDG--G-GGHV	388
EPO	QI--PGARFETNETLPLREGDRASELLNARHELTGVPNRHSAAV---FDWF--N-AGHF	396
EUGO	KI--PGARFFTTHEER---DDRGGHVLQDRHKINNGIPSLDELQL---DWVP--N-GGHI	391
	.. * . * .	
PinH	WFSPVI PRDGAEVLKINEVLGTEARRLGIPLIFAMIVPVPSWERSFTFIPLFISEDPAQ	472
PCMH	WFAPVSEARGSECKKQAAAMAKRVLHKYGLDYVAEFIV--APRDMMHVIDVLYDRTNPPE	450
EUGH	WFAPVAQVKQGEAELQVKLAQRVLAKHNLDTAGFAI--GWRDLHHIIDVLYDRNNAAEE	448
nsVAO	WFAPVAAARGVEAERQTA LAKEIVEKHGFDYTAAYAI--GWRDLHHIIALLFDKADPTQ	476
VAO	FFSPIAKVSGEDAMMQYAVTKKRCQEAGLDFIGFTFTV--GMREMHHCIVFNKKDLIQ	480
VAD	GFSVPSPITGKDAIKQYNNMVSRRVREYGFDMGLLAI--GWRDLHHTVIVYDKDPDE	445
EPO	FYAPVSAPS GEDA AKQYEDTKRISDDHGIDYLAQFII--GLREMHHCILPLYDTADPAS	453
EUGO	GFSVPVSAPDGREAMKQFEMVRNRANEYNKDYAAQFII--GLREMHHVCLFIYDTAYPEA	448
	: * : * : . : : . : . . . : :	
PinH	NKRSREVFRHLIKVAADNGWGEYRTAPTFQADVMDTYSFGDHALLRFHESIKDAVDPKGITKRADACFNELLDEFEGYAVYRVNTRFQDRAVQSYGPV--KRKLEHAIKRAVDPNNIKKRAYACFDELIEVFAAEGFASYRTNIAFMKDVKAKKFGST--NMHVNQQIKKALDPNGIEQKADACYRELVTRFGAQGWASYRTGVNSMDLVAQQYGEV--NRDFNRTLKRAIDPNGIKRKVQWLMRTLIDDCAA NGWGEYRTLAFMDQIMETYWNWNSSFLRFNEVLKNAVDPNGIRRKLDLFNII VDAAAEGYGEYRTHIRYMDRIAKTYSWNDNALWKMHETIKDALDPNGIRKETLDMTRELIRAGAE EGYGIYRAHNVLADQVAETYSFNNHIQRRSHERIKDALDPNGIREEILQMTKV LVREAAEAGYGEYRTHNALMDVMATFNWGDGALLKFHEKIKDALDPNGI	532
PCMH	.. * : * : . : . : . : * : * : * : * : .	507
EUGH		505
nsVAO		533
VAO		540
VAD		505
EPO		513
EUGO		508
PinH	LSPGRYGIWPKHLRDHKRYKGGSV 557	
PCMH	LAPGRSGIDLNND----- 521	
EUGH	LAPGKSGIHLPD----- 517	
nsVAO	LSPGKSGIHP----- 543	
VAO	IAPGKSGVWPSQYSHVTWKL---- 560	
VAD	LAPGKSGIWGKNRRKA----- 521	
EPO	LNP GKGSIWPERLRNK----- 529	
EUGO	IAPGKSGIWSQRFRGQNL----- 526	
	. * * . *	

	PinH	PCMH	EUGH	nsVAO	VAO	VAD	EPO	EUGO
PinH	100.00							
PCMH	34.71	100.00						
EUGH	32.02	53.79	100.00					
nsVAO	36.17	44.94	54.86	100.00				
VAO	37.96	32.43	35.21	36.36	100.00			
VAD	41.36	43.47	40.90	42.91	46.33	100.00		
EPO	36.85	35.47	36.45	36.27	41.84	41.92	100.00	
EUGO	41.43	39.49	38.94	39.96	46.45	51.45	51.53	100.00

Figure S2. Sequence alignment and identities of pinoresinol hydroxylase from *unclassified Pseudomonas* (PinH), *p*-cresolmethylhydroxylase from *Pseudomonas putida* (PCMH), eugenol hydroxylase from *Pseudomonas* sp, (EUGH), vanillyl alcohol oxidase from *Novosphingobium* sp (nsVAO), vanillyl-alcohol oxidase from *Penicillium simplicissimum* (VAO), vanillyl-alcohol dehydrogenase from *Marinicaulis flavus* (VAD), 4-ethylphenol oxidase from *Gulosibacter chungangensis* (EPO) and eugenol oxidase from *Rhodococcus jostii* (EUGO). The critical residues, listed in **Table 1**, are highlighted

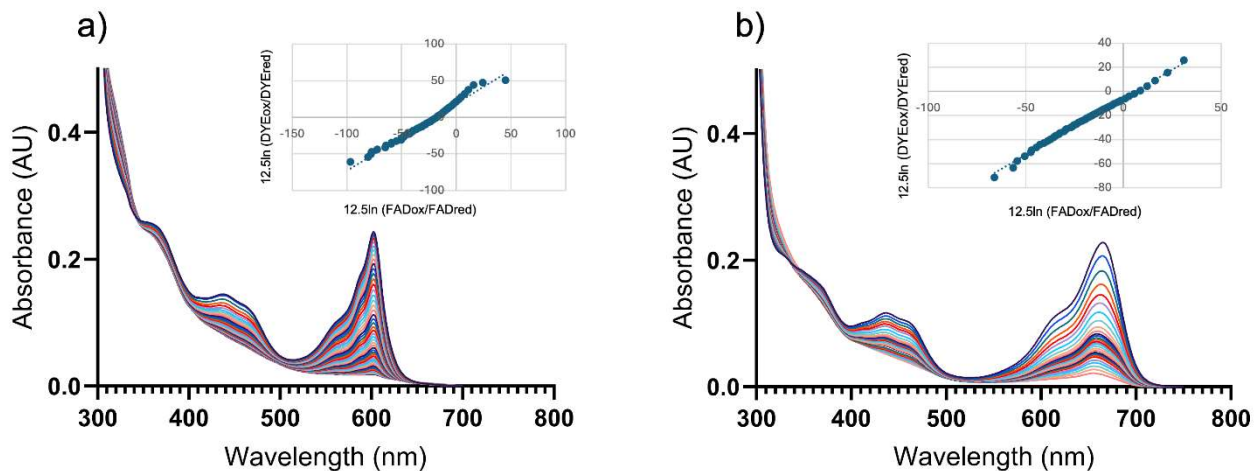
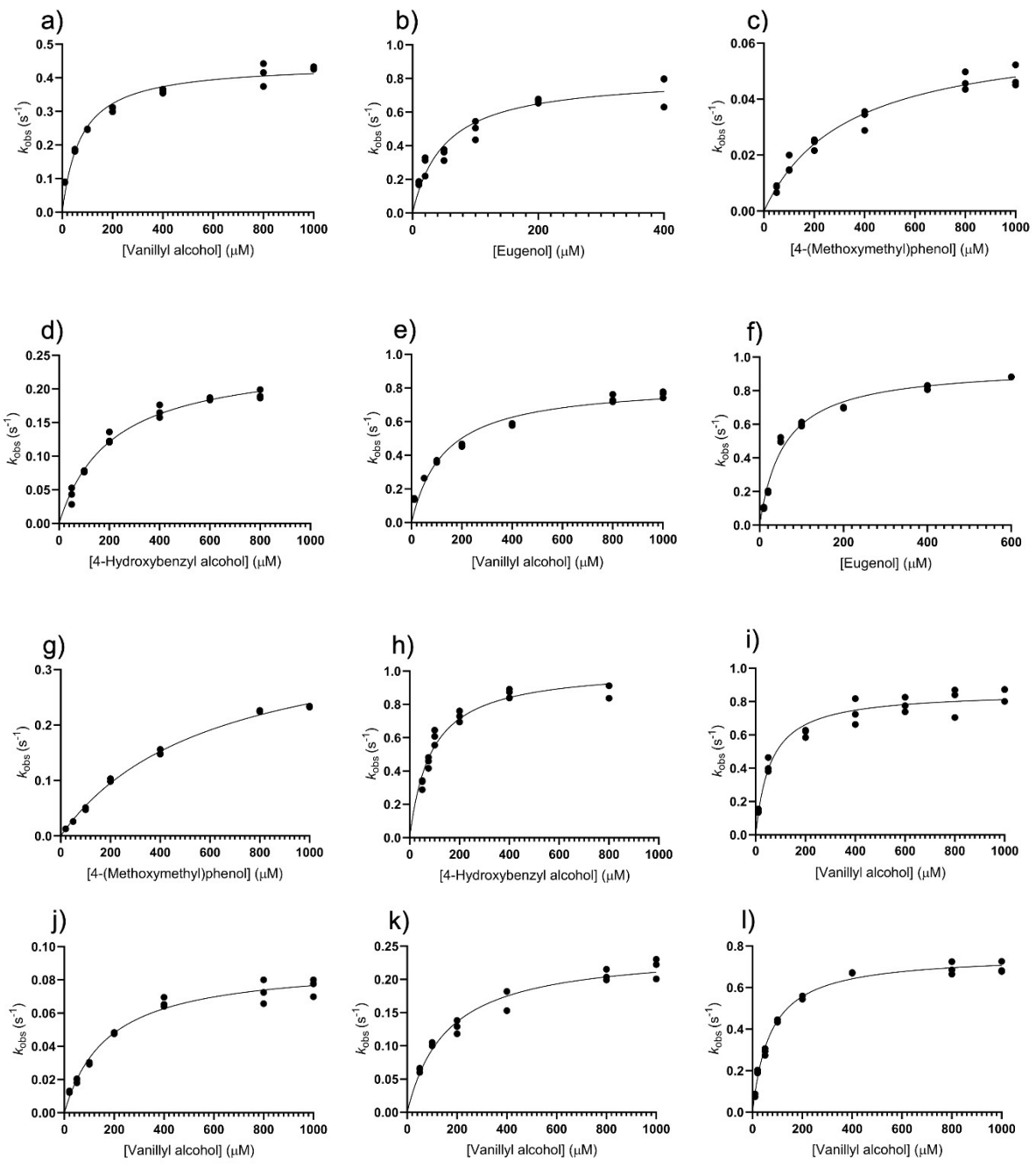


Figure S3. Determination of the midpoint redox potential (E_m) of VAD using the xanthine/xanthine oxidase method. Spectral changes observed for the determination of the midpoint redox potential of (a) wild type VAD using methylene blue as dye; (b) P151L using thionine acetate as dye. The spectra show the simultaneous reduction of the protein and the dye. They were measured every minute for 60 minutes. The inset shows a plot in which the $\log[(\text{Ox}_{\text{dye}})/(\text{Red}_{\text{dye}})]$ is on the Y-axis, and $\log[(\text{Ox}_{\text{enzyme}})/(\text{Red}_{\text{enzyme}})]$ is on the X-axis. The redox potential of the wild-type enzyme and P151L was found to be $+82 \pm 2$ mV and $+6 \pm 1$ mV, respectively.



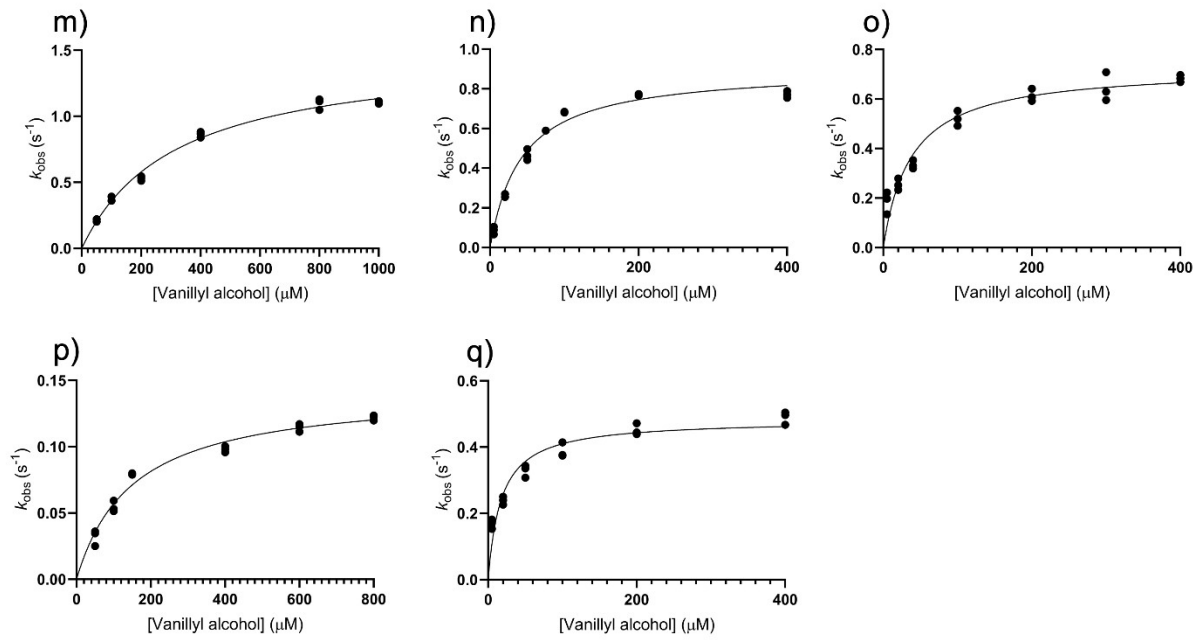


Figure S4. Steady-state kinetics experiments on VAD. Wild-type VAD with (a) vanillyl alcohol and 2,6-dichlorophenolindophenol (DCPIP), (b) eugenol and DCPIP, (c) 4-(methoxymethyl)phenol and DCPIP, (d) 4-hydroxybenzyl alcohol and DCPIP. P151L with (e) vanillyl alcohol, (f) eugenol, (g) 4-(methoxymethyl)phenol, (h) 4-hydroxybenzyl alcohol. (i) P151G with vanillyl alcohol. j) P151V with vanillyl alcohol. (k) P151I with vanillyl alcohol. (l) P151L with vanillyl alcohol and DCPIP. (m) P151G with vanillyl alcohol and DCPIP. (n) P151V with vanillyl alcohol and DCPIP. (o) P151I with vanillyl alcohol and DCPIP. (p) P151N with vanillyl alcohol and DCPIP. (q) P151T with vanillyl alcohol and DCPIP. $n = 3$ independent experiments, individually plotted as dots.

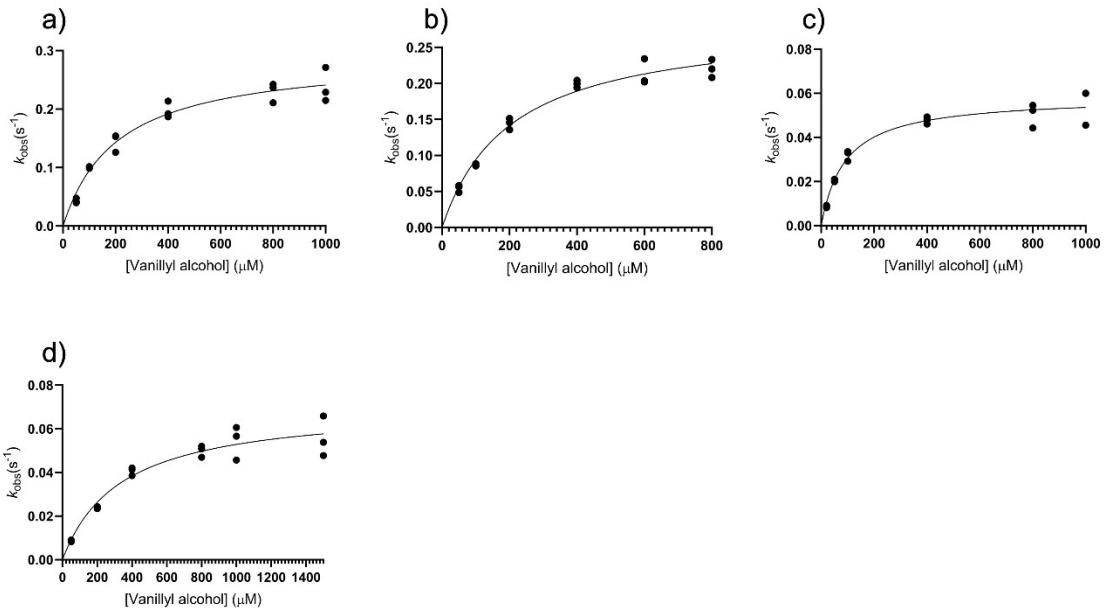


Figure S5. Steady-state kinetics experiments on nsVAO. (a) Wild type enzyme with vanillyl alcohol, (b) T181D with vanillyl alcohol, (c) wild type with vanillyl alcohol and cytochrome c. (d) T181D with vanillyl alcohol and cytochrome c. n = 3 independent experiments, individually plotted as dots.

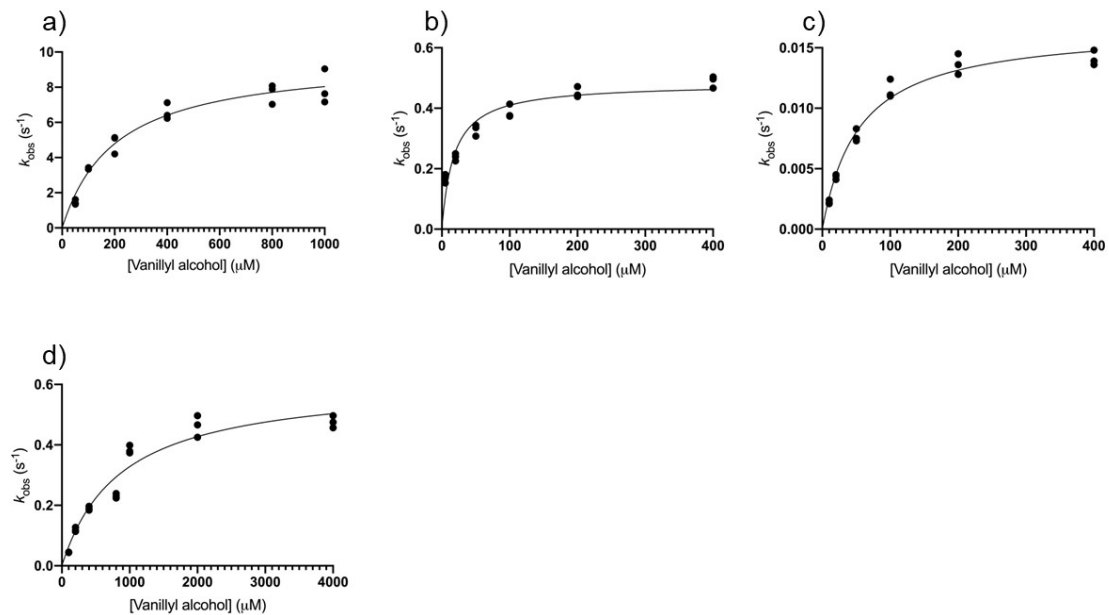


Figure S6. Steady-state kinetics experiments on EUGO from *Rhodococcus jostii* RHA1. (a) Wild type enzyme with vanillyl alcohol, (b) wild type with vanillyl alcohol and DCPIP, (c) EUGO L152P with vanillyl alcohol, (d) EUGO L152P with vanillyl alcohol and DCPIP.

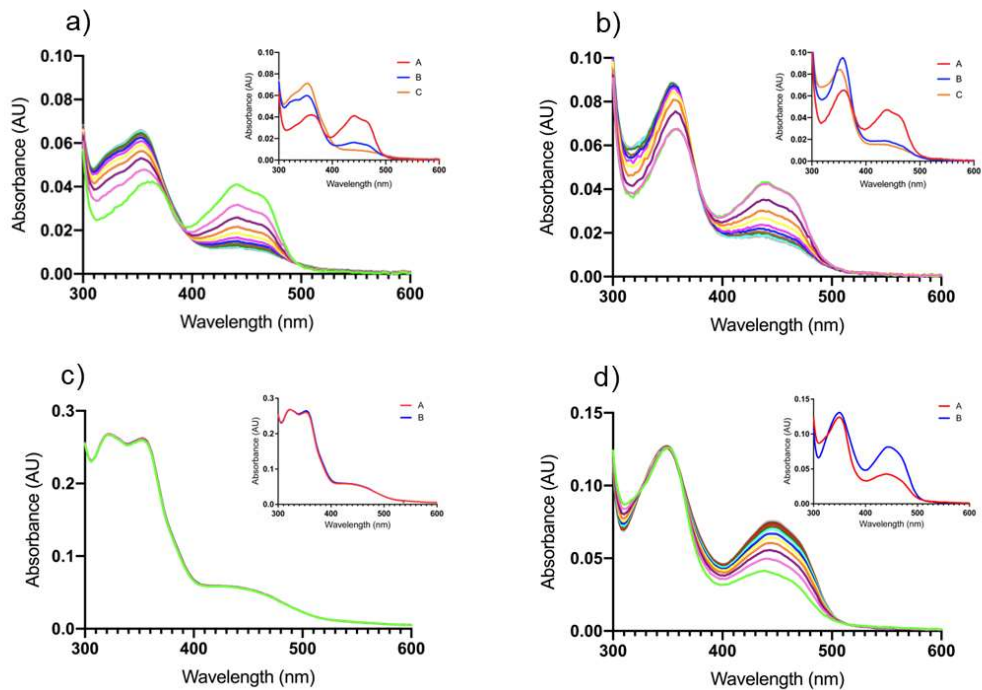


Figure S7. Spectral changes observed through stopped-flow apparatus. (a) Anaerobic mixing of wild-type VAD (5 μM) with vanillyl alcohol (400 μM) and (b) P151L (5 μM) with vanillyl alcohol (1000 μM). Spectral scans are shown from 0 to 10 s with intervals of 1 s for the wild-type enzyme, and from 0 to 20 ms with intervals of 2 ms for P151L. The data were fit with two exponential functions ($A \rightarrow B$, $B \rightarrow C$). The insets show the deconvolution of the spectral scans for A , B and C . In the B state, the enzyme is almost completely reduced and the k_{red} values listed in **Table 3** refer to the $A \rightarrow B$ conversion rates. (c) Vanillyl alcohol-reduced wild-type VAD (20 μM) upon mixing with oxygen and (d) vanillyl alcohol-reduced P151L (10 μM) upon mixing with oxygen. Spectral scans are shown from 0 to 10 s with intervals of 1 s for the wild-type enzyme, and from 0 to 2 s with intervals of 0,2 s for P151L. The data were fit with one exponential function ($A \rightarrow B$) as listed in **Table 4**. The insets show the deconvolution of the spectral scans for A and B .

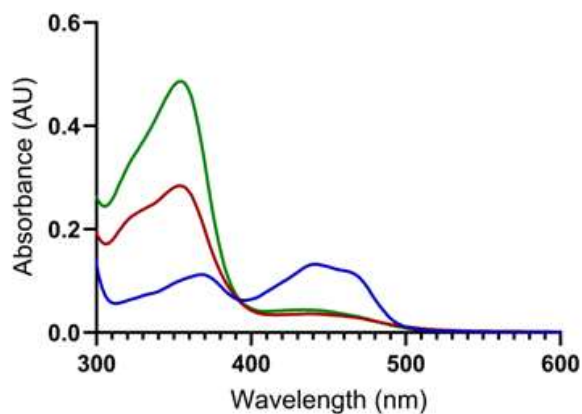


Figure S8. Enzyme-monitored turnover experiment. Spectral changes observed upon aerobic mixing wild type and P151L VAD (12 μ M) with 2.5 mM vanillyl alcohol. The spectrum of the initial oxidized wild-type enzyme is in blue. The spectrum of P151L would be indistinguishable and is not shown for clarity. The spectra of the wild-type and P151L proteins after 10 s incubation are in red and blue, respectively.

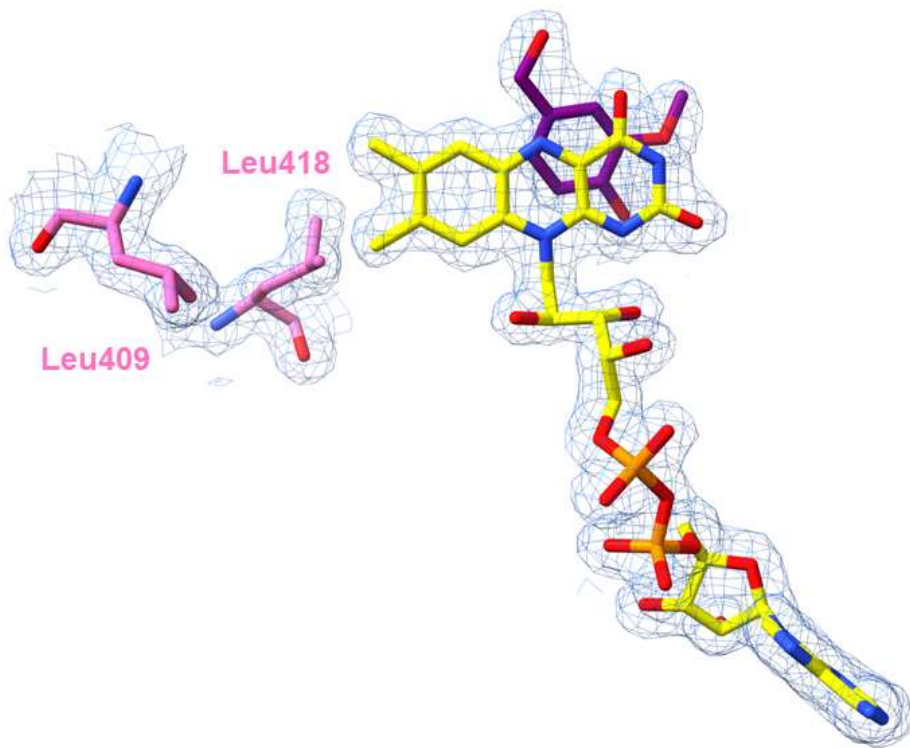


Figure S9. The electron density of the flavin and surrounding residues in nsVAO. The weighted 2Fo-Fc map is contoured at 1.2 σ level.

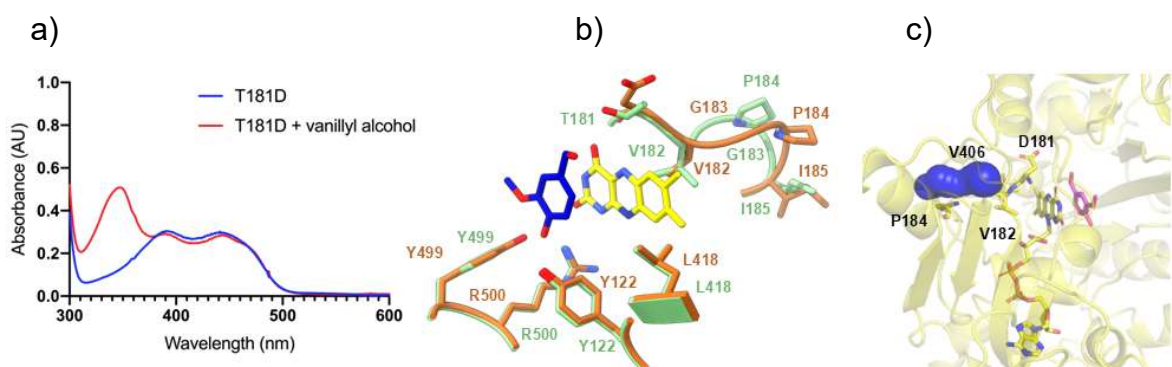


Figure S10. Properties of nsVAO T181D mutant. (a) Incubation of T181D (30 μM) with vanillyl alcohol (45 μM). The spectra before substrate addition and after 30-minute incubation are in blue and red, respectively. Vanillin, formed upon vanillyl alcohol oxidation, has an absorbance peak at 340 nm ($\epsilon=14000 \text{ M}^{-1}\cdot\text{cm}^{-1}$). (b) Structural comparison between wild type (green carbons) and T181D (dark orange carbons) nsVAOs. (c) Accessibility of the flavin N5-C4a locus. Compared to the wild-type nsVAO (Figure 8c), there is a narrowing of the tunnel leading to the flavin re side, as revealed by the mutant's crystal structure

Table S1a. Data collection and refinement statistics of VAD: wild type, P151L, P151I and VAD P151V.

	Wild Type	P151L	P151I	P151V
PDB code	8S7P	8S7U	8S7Q	8S7W
Space group	C222 ₁	P4 ₁ 2 ₁ 2	P2 ₁ 2 ₁ 2 ₁	P2 ₁ 2 ₁ 2 ₁
Unit cell axes (Å)	90.14, 143.22, 287.75	138.495, 138.495, 180.947	100.443, 113.338, 130.168	100.62, 114.64, 130.71
Unit cell angles (°)	90, 90, 90	90, 90, 90	90, 90, 90	90, 90, 90
Resolution (Å)	67.49– 2.35	47.31– 1.80	52.01– 2.40	49.86– 2.10
R_{merge}	0.166 (3.295)	0.146 (2.885)	0.198 (1.032)	0.159 (1.132)
CC _{1/2}	0.998 (0.488)	0.999 (0.390)	0.994 (0.664)	0.989 (0.394)
Completeness (%)	100.0 (99.6)	99.7 (100.0)	99.7 (96.9)	98.8 (99.1)
Unique reflections	77772 (4521)	161652 (7961)	58641 (4368)	87358 (4434)
Multiplicity	21.3 (16.1)	13.5 (13.4)	8.8 (7.8)	4.3 (4.1)
Overall $I/\sigma(I)$	12.6 (0.8)	11.8 (0.9)	9.1 (2.1)	8.4 (1.6)
Protein residues	1556	1038	1038	1038
FAD molecules	3	2	2	2
Ligand	-	-	-	-
Water molecules	48	718	358	589
R/R_{free} (%)	22.8 /27.9	15.5/18.0	17.8/23.1	17.2/20.9
Rms bond length	0.001	0.001	0.001	0.001
Rms bond angle	0.518	1.497	0.488	1.343
Ramachandran outliers (%)	0.2	0.1	0.2	0.0
Average B-factor	57.0	30.0	34.0	28.0

Table S1b. Data collection and refinement statistics of VAD: P151L, P151T, P151N and P151G.

	P151L with eugenol	P151T	P151N	P151G
PDB code	8S7N	8S7R	8S7T	8S7S
Space group	P4 ₁ 2 ₁ 2	C222 ₁	C222 ₁	C222 ₁
Unit cell axes (Å)	139.02, 139.02, 181.06	91.949 144.451 286.785	89.525 142.426 286.436	90.804 144.145 289.452
Unit cell angles (°)	90, 90, 90	90, 90, 90	90, 90, 90	90, 90, 90
Resolution (Å)	49.20– 1.80	143.39– 1.90	143.22– 2.10	64.60 – 2.50
R_{merge}	0.194 (3.735)	0.066 (1.253)	0.139 (2.349)	0.202 (3.274)
CC _{1/2}	0.998 (0.388)	0.991 (0.423)	0.999 (0.553)	0.997 (0.605)
Completeness (%)	100.0 (100.0)	97.8 (98.7)	100.0 (100.0)	100.0 (100.0)
Unique reflections	163464 (8025)	146187 (7204)	106762 (5214)	66056 (4381)
Multiplicity	13.5 (13.3)	3.7 (3.8)	20.1 (20.7)	22.8 (23.6)
Overall $I/\sigma(I)$	11.0 (0.9)	9.2 (1.1)	14.3 (1.5)	12.5 (1.2)
Protein residues	1038	1554	1553	1554
FAD molecules	2	3	3	3
Ligand molecules	2	-	-	-
Water molecules	917	468	292	242
R/R_{free} (%)	15.8 /18.4	19.4/ 23.5	18.4/23.2	19.2/25.2
Rms bond length	0.001	0.001	0.001	0.001
Rms bond angle	1.485	0.456	0.463	0.506
Ramachandran outliers (%)	0.0	0.0	0.1	0.2
Average B-factor	27.0	46.0	50.0	57.0

Table S1c. Data collection and refinement statistics of nsVAO.

	nsVAO with vanillyl alcohol	T181D with vanillin
PDB code	9FFK	9FGE
Space group	P22 ₁ 2 ₁	P22 ₁ 2 ₁
Unit cell axes (Å)	90.84, 96.77, 129.11	91.33 97.82 129.61
Unit cell angles (°)	90, 90, 90	90, 90, 90
Resolution (Å)	90.85 – 1.70	78.20 – 1.60
R_{merge}	0.162 (2.466)	0.15 (1.476)
CC _{1/2}	0.999 (0.707)	0.998 (0.793)
Completeness (%)	99.7 (99.7)	99.6 (99.3)
Unique reflections	125029 (6098)	152440 (7444)
Multiplicity	20.0 (18.6)	9.3 (9.1)
Overall $I/\sigma (I)$	10.1 (1.3)	8.8 (1.6)
Protein residues	1002	1002
FAD molecules	2	2
Ligand molecules	2	2
Water molecules	558	772
R/R_{free} (%)	22.3 /25.4	17.5/20.4
Rms bond length	0.002	0.001
Rms bond angle	1.449	0.579
Ramachandran outliers (%)	1	0.2
Average B-factor	27.0	18.0

Table S2. Genetic context of VAD from *Marinicaulis flavus* and VAO from *Novosphingobium* sp.

	GenBank Accession Code	Annotation
Upstream genes	WP_104830656.1	UbiD family decarboxylase
	WP_104830657.1	Hypothetical protein
	WP_104830658.1	Pilus assembly protein TadG-related protein
	WP_104830659.1	Pilus assembly protein
	WP_104830660.1	Pilus assembly protein
	WP_207764815.1	Putative cytochrome c
VAD	WP_104830661.1	FAD-binding oxidoreductase
Downstream genes	WP_133162311.1	Hypothetical protein
	WP_104830663.1	ATPase
	WP_104830664.1	Hypothetical protein
	WP_104830665.1	Hypothetical protein
	WP_104830666.1	Glutathione S-transferase family protein
	WP_104830667.1	Glutathione-dependent disulfide-bond oxidoreductase

	GenBank Accession Code	Annotation
Upstream genes	WP_124809343.1	Glycogen/starch/alpha-glucan phosphorylase
	WP_124809344.1	1,4-alpha-glucan branching protein GlgB
	WP_124809345.1	Glucose-1-phosphate adenylyltransferase
	WP_124809346.1	Glycogen synthase GlgA
	WP_124809347.1	Alpha-D-glucose phosphate-specific phosphoglucomutase
	WP_223806624.1	Glycogen debranching protein GlgX
nsVAO	WP_124809348.1	FAD-binding oxidoreductase
Downstream genes	WP_124809349.1	Putative cytochrome c
	WP_190287233.1	TetR/AcrR family transcriptional regulator
	WP_124809351.1	Alpha/beta hydrolase
	WP_124809352.1	DUF2334 domain-containing protein
	WP_223806625.1	Hypothetical protein
	WP_124809353.1	Glycosyltransferase

Table S3. Steady state kinetic parameters of P151L VAD

VAD	Substrate	O ₂		
		<i>k</i> _{cat} (s ⁻¹)	K _M (μM)	<i>k</i> _{cat} /K _M (s ⁻¹ mM ⁻¹)
P151L	Vanillyl alcohol	0.83±0.05	131.9±30.4	6
P151L	Eugenol	0.92±0.04	55±8.8	17
P151L	4-Hydroxy benzylalcohol	1.02±0.03	86.74±9.1	12
P151L	4-Methoxy methylphenol	0.38±0.02	600±70	0.6

Measured at 25 °C in 50 mM potassium phosphate pH 7.5, 150 mM NaCl. Data are shown as average values ± standard deviation. n = 3 independent experiments. No activity was detected on *p*-cresol.

Supplementary Table 4. Primers used for quick change mutagenesis

Primer name	Sequence
VAD_P151Lfw	gtgccggacacctgggctggggtagtgtggcgg
VAD_P15Lrv	accccagcccagggtccggcacatcgatccata
VAD_P151Vfw	ccggacgtggctggggtagtgtg
VAD_P151Vrv	ccagcccacgtccggcacatcgatc
VAD_P151Ifw	ccggacattggctggggtagtgtg
VAD_P151Irw	ccagccaatgtccggcacatcgatc
VAD_P151Gfd	gtgccggacggcggctggggtagtgtggcgg
VAD_P151Grv	accccagccgcgtccggcacatcgatccata
VAD_P151Nfw	gtgccggacaacggctggggtagtgtggcgg
VAD_P151Nrv	accccagccttggtccggcacatcgatccata
VAD_P151Tfw	ccggacaccggctggggtagtgtg
VAD_P151Trv	ccagccgggtccggcacatcgatc
nsVAO_T181Dfw	acgtcccagatgtggcccgattgcatctccag
nsVAO_T181Drv	cgggcccacatctgggacgtcaatccaaaggga

EUGO_L152Pfw	gaccggatgggcagcgtg
EUGO_L152Prv	ccatcccgggtcggcacagtc